

The Non–Monotonic Dependence of Supernova and Remnant Formation on Progenitor Rotation

Shizuka Akiyama, J. Craig Wheeler

Astronomy Department, University of Texas, Austin, TX 78712

shizuka@astro.as.utexas.edu, wheel@astro.as.utexas.edu

ABSTRACT

Traditional models of core collapse suggest the issue of successful versus failed supernova explosions and neutron star versus black hole formation depends monotonically on the mass (and metallicity) of the progenitor star with mass above some cutoff leading to black holes with or without attendant supernova explosions. Here we argue that the issue of success or failure of the explosion or other possible outcomes may depend non–monotonically on the rotation of the progenitor star even at fixed progenitor mass and composition. We have computed “shellular” models of core collapse for a star of $15 M_{\odot}$ with initial central angular velocity, Ω_0 , in the range $0.1 - 8 \text{ rad s}^{-1}$ until a few hundred ms after bounce to explore qualitative trends. The model with $\Omega_0 = 4 \text{ rad s}^{-1}$ gives the maximum post–bounce rotation with rotation comparable to that necessary for secular or dynamical instability to occur. Models with $\Omega_0 > 4 \text{ rad s}^{-1}$ bounce at sub–nuclear density with $\gamma \sim 4/3$ and subsequently slowly contract. The non–monotonic behavior will be manifested in the rotation of the proto–neutron star and hence in the strength of the associated magnetic field that will be generated by shear in that rotating environment. We estimate that our maximally rotating and shearing models generate toroidal fields approaching or exceeding 10^{17} G , strengths nearing dynamical significance. One implication of this nonmonotonicity is that the process of rotating, magnetic core collapse may itself provide a filter to select specific outcomes from the distribution of initial rotation states. A possible outcome is black hole – neutron star – black hole with increasing initial angular momentum of the progenitor. Within the regime of successful explosions leaving neutron stars behind, a subset may spin rapidly enough, either initially or during the subsequent de–leptonization contraction phase, to drive an $\alpha - \Omega$ dynamo and hence produce the large dipole field associated with magnetars.

Subject headings: pulsars: general – pulsars: magnetars – stars: magnetic fields
– stars: rotation – supernovae: general – supernovae: core collapse

1. Introduction

The collapse of the core of a massive star can lead to a number of possible outcomes: an explosion leaving behind a neutron star, frequently observationally manifested as a pulsar; an explosion leaving behind an especially strongly magnetized neutron star, a magnetar (Duncan & Thompson 1992; Kouveliotou et al. 1999); a black hole associated with an otherwise successful explosion; or complete collapse to a black hole with little or no mass ejection or light output. Classical Type II supernovae may be one extreme of this distribution of properties, gamma-ray bursts another.

Traditional, spherical or nearly spherically-symmetric models of core collapse have led to the widespread assumption that the outcome of core collapse depends monotonically on the mass of the progenitor star. The assumption, implicit or explicit, is that with increasing binding energy and overburden in more massive stars, the explosion becomes more difficult and hence black hole formation though fall-back or complete collapse becomes more likely (Burrows 1988; Fryer 1999; Fryer & Kalogera 2001).

The physics that dictates the reversal of core collapse into an explosion is not yet fully understood. Neutrino processes undoubtedly play a major role (Rampp & Janka 2000, 2002; Liebendörfer et al. 2001a,b; Mezzacappa et al. 2001; Thompson et al. 2005), but the discovery of ubiquitous asymmetries in core collapse supernovae (Wang et al. 1996, 2001, 2002, 2003; Leonard et al. 2000, 2001, 2002) and the success of jet-induced models to form such asymmetries (Khokhlov et al. 1999; Khokhlov & Höflich 2001; Höflich, Khokhlov, & Wang 2001) and effects on the nucleosynthesis (Maeda & Nomoto 2003) have brought new focus to the question of whether rotation (Fryer & Heger 2000; Müller et al. 2004; Fryer & Warren 2004; Ott et al. 2004) and magnetic fields (Wheeler et al. 2000; Wheeler, Meier, & Wilson 2002; Kotake et al. 2004; Yamada & Sawai 2004) play an important part in the explosion process. In particular, Akiyama et al. (2003) showed that the magnetorotational instability (MRI; Balbus & Hawley 1998) will be a ubiquitous effect in the differentially-rotating structure associated with a newly formed neutron star where predominantly toroidal fields of $\sim 10^{15} - 10^{16}$ G are expected. Thompson et al. (2005) explored the possibility that heating from magnetic dissipation may boost that from neutrino deposition.

In general, more rapid rotation of the new-born neutron star will lead to greater shear and to production of larger magnetic fields, whatever their influence on the outcome of the

explosion. On the other hand, given the plethora of single and binary star evolutionary paths that can influence the progenitor rotational evolution, it is difficult to believe that all stars evolve to just the right rapidly rotating pre-collapse state (Langer 2004). There must be a distribution of initial angular momenta of the progenitor stars, of the pre-collapse cores, and of the neutron stars. Here we argue that the processes of collapse, rotation, shear, and magnetic field generation may provide the filter to select specific outcomes from this distribution of initial rotation states. In particular, we argue that the final angular velocity that determines the shear and hence the strength of the magnetic field generated by the MRI will not vary monotonically with the initial rotation speed of the pre-collapse core. This, in turn, suggests that the outcome of core collapse at a single mass may depend in a non-monotonic manner on the initial angular momentum of the pre-collapse core.

In §2 we outline the basic nature of the argument and present a simple analytic model to show the general trend. In §3 we present numerical results from a “shellular” collapse with a centrifugal potential to extend the argument. Section 4 gives a summary and conclusions.

2. Qualitative Non-monotonic Behavior and a Simple Model

The basic thrust of our argument is that the final outcome of core collapse will naturally lead to a non-monotonic behavior of the neutron star rotational velocity, the shear, and the magnetic field with the initial angular momentum of the core. This is because for low initial angular momentum the outcome will be very similar to that for non-rotating models, whatever that is. As the initial angular momentum increases, so will the resulting rotation rate of the neutron star. If the initial angular momentum increases sufficiently, however, centrifugal effects will prevent the neutron star from becoming as compact (at least along the equator) and hence the angular velocity of the neutron star will be less. The result is that the angular velocity and hence the shear and associated magnetic field may have a distinct maximum as the initial angular momentum of the pre-collapse core is increased. This could single out a rather narrow range of initial angular momenta at which the angular velocity, shear, and resulting magnetic field will be a maximum.

The basic behavior can be illustrated with a simple model. If we treat the effects of rotation as an effective centrifugal potential, then pressure gradients in the post-bounce quasi-static proto-neutron star core can be described by:

$$\nabla P = -\rho \nabla \Phi_G (1 - \epsilon), \quad (1)$$

where

$$\epsilon = \left| \frac{\Phi_c}{\Phi_G} \right| \sim \frac{L^2}{GM^3 R} \quad (2)$$

is the absolute value of the ratio of the centrifugal potential, Φ_c , to the gravitational potential and L is the initial angular momentum of the pre-collapse core which is assumed to be conserved, so that $L \sim MR^2\Omega$ where M is the mass of the neutron star, R its radius, and Ω its angular velocity.

To simplify the argument, we consider eq. (1) in terms of characteristic quantities and write,

$$P \sim \rho\Phi_G(1 - \epsilon). \quad (3)$$

If we consider a simple polytropic equation of state, $P = K\rho^\gamma$, then with $\rho \sim M/R^3$ in eq. (3) we find

$$\left(\frac{R}{R_0}\right)^{3\gamma-4} \sim (1 - \epsilon)^{-1}, \quad (4)$$

where R_0 is the radius of the neutron star in the absence of rotation. Since $\Omega \sim L/MR(L)^2$, eq. (4) is an implicit equation for Ω as a function of L .

To see the form of $\Omega(L)$, we assume that ϵ is a small quantity. With the appropriate Taylor expansion we find

$$R^{3\gamma-3} - R_0^{3\gamma-4}R \sim \frac{R_0^{3\gamma-4}L^2}{GM^3}. \quad (5)$$

If we further assume that $R = R_0(1 + \eta)$ where η is another small quantity we find

$$\eta = \frac{L^2}{3(\gamma - \frac{4}{3})GM^3R_0}. \quad (6)$$

Note that this factor by which the radius is amplified by rotation can be exaggerated compared to the amplitude of the parameter ϵ because of the factor of $\gamma - \frac{4}{3}$ in the numerator. We will explore a related effect in the numerical models presented below.

We then define a characteristic angular momentum, L_c , as

$$L_c = \left[3\left(\gamma - \frac{4}{3}\right)GM^3R_0\right]^{1/2}, \quad (7)$$

where L_c is related to, but not identical with, the Keplerian angular momentum. With the definition of eq. 7, we can write

$$\Omega \sim \frac{L}{MR_0^2 \left[1 + \left(\frac{L}{L_c}\right)^2\right]^2}. \quad (8)$$

We thus see that for $L \ll L_c$, Ω increases with L , but that as L becomes comparable to and then exceeds L_c , Ω will tend to decrease with further increase in L . Eq. 8 is not

applicable in the regime $L \gtrsim L_c$ because of the small parameter approximations made, but the general trend is clear. To avoid these small parameter approximations a numerical model is needed, to which we now turn.

3. Time-Dependent Behavior with Varying Initial Angular Momentum

In order to demonstrate the simple model described above, we have simulated the collapse of an iron core of a $15 M_\odot$ progenitor model with a one-dimensional flux-limited diffusion code (Myra et al. 1987). We assign an initial rotational velocity profile to the one-dimensional initial iron core, and calculate the subsequent angular velocity by assuming conservation of angular momentum in each mass shell. The angular momentum in the collapsing core can safely be assumed to be conserved until core bounce according to the two-dimensional simulations of Yamada & Sawai (2004) (see their Fig. 11). We have modified the original code to include the centrifugal potential in accord with eqs. 1 and 2 in order to assess rotational feedback on the dynamics. Specifically, we have added a term $+r\Omega^2$ to the gravitational acceleration, $-GM_r/r^2$, in the momentum equation. We keep in mind that our calculations presented here after bounce and with significant rotational energy are not realistic because of our assumptions of spherical symmetry and conservation of angular momentum. Nevertheless we have identified some interesting trends that can be explored with multidimensional simulations.

The rotational profile employed here is of the form (Mönchmeyer & Müller 1989)

$$\Omega(r) = \Omega_0 \frac{R^2}{r^2 + R^2}, \quad (9)$$

where $R = 10^8$ cm, and Ω_0 is the initial central value of the rotational velocity profile. We study the non-monotonic behavior of post-collapse rotation by varying the value of Ω_0 . A total of 14 models have been computed with values of Ω_0 varying from 0.1 to 8.0 s^{-1} (see Table 1). The models are indicated by the value of Ω_0 , i.e. m0.1 for the model with $\Omega_0 = 0.1 \text{ rad s}^{-1}$. The corresponding values of the ratio of rotational energy to absolute value of the gravitational energy $T/|W|$ are given in Table 1 and range from $8.58 \times 10^{-4}\%$ to 5.49%. Maclaurin spheroids are unstable to secular instability when $T/|W| > 14\%$ and to dynamical instability when $T/|W| > 27\%$ (Tassoul 1978). The value of $T/|W|$ for the onset of secular instability in more realistic situations is estimated to be comparable to the value for Maclaurin spheroids (Shapiro & Teukolsky 1983; however see §4 for a discussion of the bar mode instability). Therefore our initial rotational profiles are stable to the secular instability even for our most rapidly rotating model. The amplitude of the centrifugal potential is small for the less rapidly rotating models in relative terms compared to the gravitational

potential and the ambient pressure gradients. As shown in Fig. 1, characteristic values of the centrifugal potential for models with $\Omega_0 \sim 1 \text{ s}^{-1}$ at bounce are $\sim 10^{-3} - 10^{-2}$ of the gravitational potential. Our most rapidly rotating models approach or exceed the conditions for instability after collapse, as will be illustrated below.

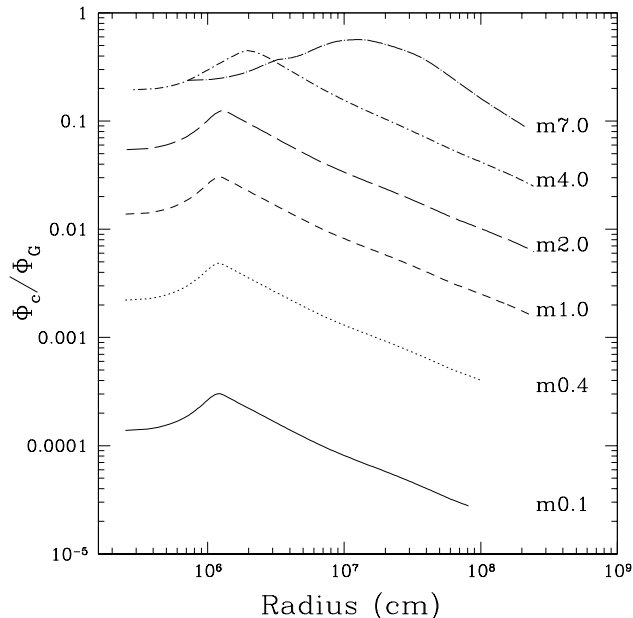


Fig. 1.— The ratio of the centrifugal potential, Φ_c , to the gravitational potential, Φ_G , as a function of radius for selected models at bounce.

For a model with modest initial rotation, the rotational velocity is most rapid at the bounce, as the core is most compact then. Fig. 2 shows the evolution of the angular velocity profile for model m0.6 and Fig. 3 displays the radius versus time profile for selected mass zones. The negative gradient in rotational velocity is greatest at the boundary between the original homologous core and the accreting matter around $2 - 3 \times 10^6$ cm. The strong negative gradient in angular velocity drives the magnetorotational instability (MRI) dynamo, and this region is expected to be associated with a strong magnetic field (Akiyama et al. 2003).

Models m5.0, m6.0, and m7.0 bounce at sub-nuclear densities due to the centrifugal potential. Centrifugal force not only results in sub-nuclear density bounce, but also delays the time to achieve bounce. Model m8.0 did not bounce by the end of our computation. Model m5.0, which is the first model in the series we computed that bounces at sub-nuclear density, bounced with a central density of $1.0 \times 10^{14} \text{ g cm}^{-3}$. As seen in Fig. 4, the structure is significantly less compact at bounce than models with lower initial rotation,

Table 1. Parameters of the models calculated.

Model	Ω_0 (s^{-1})	$T/ W (\%)$
m0.1	0.1	8.58×10^{-4}
m0.2	0.2	3.43×10^{-3}
m0.4	0.4	1.37×10^{-2}
m0.5	0.5	2.15×10^{-2}
m0.6	0.6	3.09×10^{-2}
m0.8	0.8	5.49×10^{-2}
m1.0	1.0	8.58×10^{-2}
m2.0	2.0	0.343
m3.0	3.0	0.773
m4.0	4.0	1.37
m5.0	5.0	2.15
m6.0	6.0	3.09
m7.0	7.0	4.21
m8.0	8.0	5.49

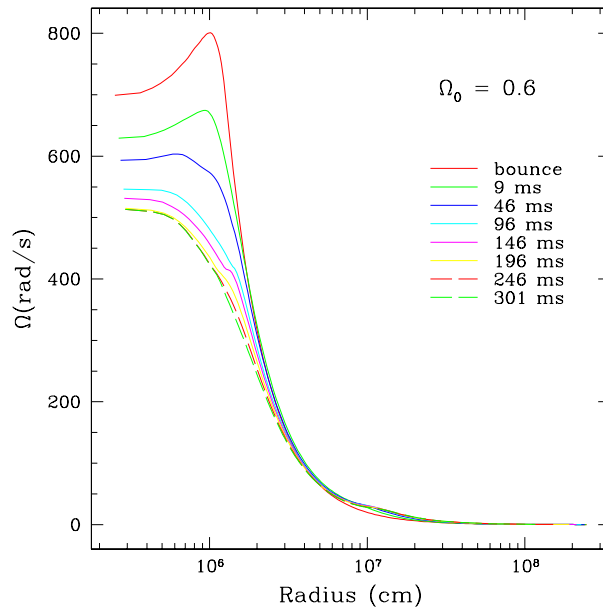


Fig. 2.— Rotational profiles of the model with $\Omega_0 = 0.6s^{-1}$ as a function of radius at elected times after bounce.

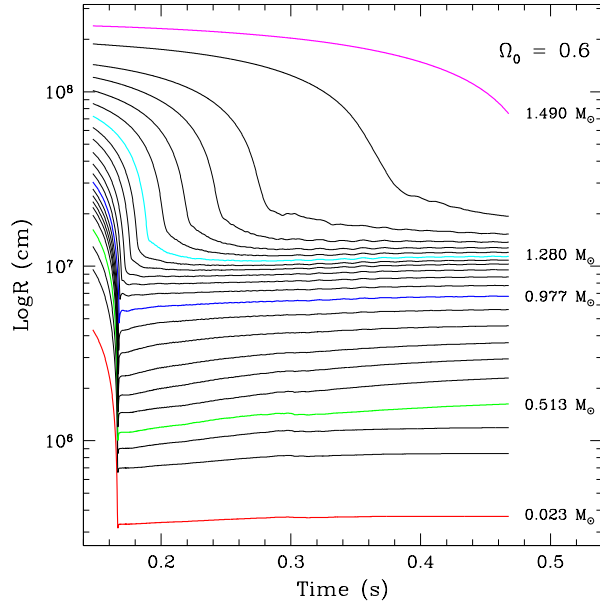


Fig. 3.— The radius versus time of selected mass zones for model m0.6.

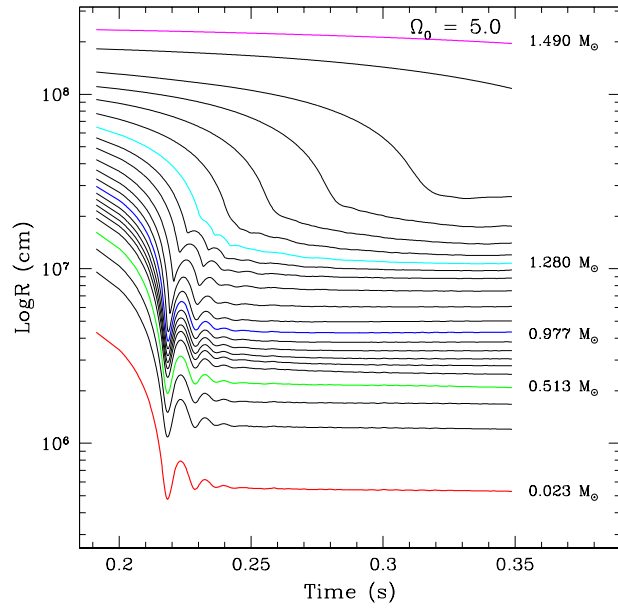


Fig. 4.— The radius versus time of selected mass zones for model m5.0.

and it oscillates a few times after bounce. This oscillation is undoubtedly an artifact of our spherical calculation, but in these calculations it is affected by the fact that the models that bounce at sub–nuclear density have $\gamma \sim 4/3$ at the time of bounce up to a radius of $\sim 10^7$ cm. The condition of essentially neutral dynamical stability makes them susceptible to radial perturbations with little energy penalty. The structure of these rotationally–supported models contracts after bounce while accreting mass from the outer layers.

The maximum value of angular velocity occurs at the boundary of the homologous core at bounce for models that bounce above nuclear density (see Fig. 2); the locus of maximum angular velocity later shifts to regions within the homologous core as the core relaxes after bounce. For sub–nuclear bounce models, the large scale angular velocity gradient is negative throughout the structure, so the innermost region of the core has the maximum value of angular velocity. For modest initial rotation, $\Omega_0 < 3 \text{ rad s}^{-1}$, the rotational velocity at bounce increases with Ω_0 , as expected from §2. More rapid rotation gives a more significant centrifugal potential after bounce. The peak in angular velocity is delayed in time for higher initial rotation and the post–bounce angular velocity increases with time for the most rapidly rotating models. For initial rotation large enough that the core bounces at sub–nuclear density due to the centrifugal effect, the rotational velocity at bounce declines with increasing Ω_0 because the core is not as compact at bounce. In our calculations, the peak of the rotational velocity at bounce corresponds to model m4.0, as shown in Fig. 5.

As the core experiences the collapse, the ratio $T/|W|$ increases (see Fig. 5) along with the increase in rotational velocity because

$$T \sim \frac{L^2}{MR^2}, \quad |W| \sim \frac{GM^2}{R}, \quad (10)$$

so that

$$\frac{T}{|W|} \sim \left(\frac{L^2}{GM^3} \right) \frac{1}{R}. \quad (11)$$

The angular momentum is nearly conserved and no mass loss is expected up to the core bounce, so that L and M are constants in our calculations and eq. (11) is a function only of R . Meanwhile, for a given radius, the ratio $T/|W|$ is larger for bigger L . While the rotational velocity at bounce has a peak with increasing Ω_0 , $T/|W|$ continues to increase according to eq. 11 (Fig. 5). Among our models that bounce at nuclear density, those with $\Omega_0 = 3.0$ and 4.0 s^{-1} may be unstable to secular and dynamical instability, respectively, since the $T/|W|$ values are close to 14% and 27%, respectively. These models are expected to depart from spherical and even axial symmetry, and our one–dimensional simulation is not adequate to follow the dynamics after bounce quantitatively. The more rapidly rotating models also have comparable or higher values of $T/|W|$ and hence should not be taken literally.

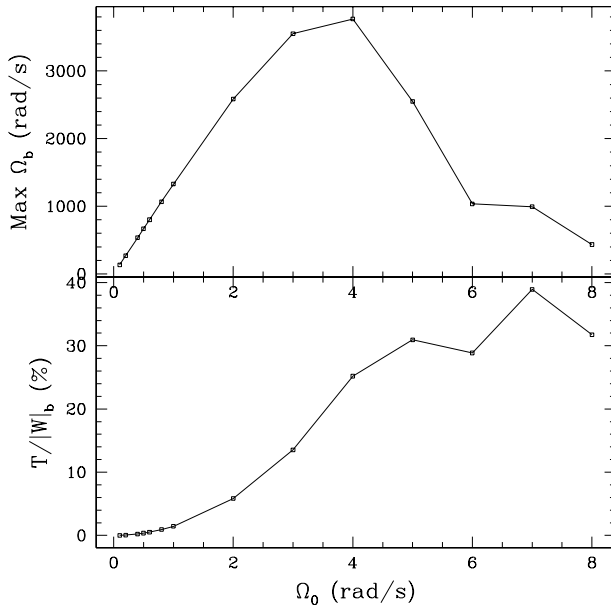


Fig. 5.— Maximum rotational velocity and $T/|W|$ at bounce as a function of initial angular velocity.

While the specifics of the non-monotonic behavior of the post-collapse angular velocity shown in Fig. 5 undoubtedly depend on the restrictions of our “shellular” model, we suggest that the general behavior will occur even in multidimensional models. We note that a peak in angular velocity as a function of initial angular momentum is observed in the two dimensional calculations of Ott et al. (2004) in their Fig. 19. The final angular velocity increases from their model with $\beta_i = 0.10\%$ to that with $\beta_i = 0.20\%$ (β is their parameter for the ratio of rotational to gravitational energy). For their model with initial differential rotation, the final angular velocity begins to decline with increasing initial angular momentum for their model with $\beta_i = 0.50\%$. Similarly, their model with initial solid body rotation exhibits a peak in final rotational velocity for models with $\beta_i = 0.50\% - 1.00\%$. Our model with maximum rotation at bounce (m4.0) corresponds to $T/|W|_i = 1.37\%$. Direct comparison of our models with those of Ott et al. (2004) is difficult since the simulations of Ott et al. (2004) are two dimensional and do not include neutrino transport, but their models clearly show a non-monotonic behavior of final angular velocity as a function of initial angular momentum. In our calculations, models that bounce at sub-nuclear densities have larger $T/|W|$ than more slowly rotating models that bounce at nuclear density, while the models in Ott et al. (2004) show a peak in $T/|W|$ (their β) for the first sub-nuclear bounce model at the time of bounce after which $T/|W|$ decreases with increasing initial rotation (see their Fig. 7). It seems unlikely that the difference is our inclusion of neutrino transport since the low densities

associated with sub–nuclear bounce will mute the neutrino production. Rather, we suspect the difference is that the two–dimensional models allow some of the gravitational potential to be converted into circulatory motion in addition to rotational motion whereas our models force rotation on shells and hence a large contribution to T . We also neglect dissipation between shells in these trial calculations, an effect that will also tend to maximize T .

Despite the limitations on our models with strong centrifugal force and high $T/|W|$, the general trend seen in our calculations can be argued by simple physics. Starting from small initial angular velocity, the larger the initial angular velocity, the larger the centrifugal force and angular velocity at bounce. When the centrifugal force is strong enough to halt the collapse before the core achieves nuclear density, the angular velocity is smaller than it would be otherwise because the core is not as compact. As the initial rotational velocity increases, the centrifugal force is stronger, and core bounce occurs at lower density and later time. This implies that there should be a peak at which the rotational velocity is rapid, but the centrifugal force is not strong enough to yield sub–nuclear bounce. Such a peak is observed in Fig. 5, and happens near $\Omega_0 = 4.0 \text{ rad s}^{-1}$ in our calculations.

4. Summary and Conclusions

There are several possible outcomes from core collapse that pertain to the nature of the explosions and the nature of the compact remnants left behind. Core collapse can result in a successful or a failed supernova explosion, and in the case of a successful explosion there are several types of supernova (Type II, Type Ib, Type Ic, etc.), and some supernovae are associated with gamma–ray bursts. The central compact remnants can be neutron stars or black holes (formed directly or by fall back) with a range of rotation rates and magnetic field strengths. Differences in outcome with respect to compact remnants are usually attributed to the mass of the progenitor core and of the envelope or to a combination of the initial mass and the metallicity (through mass loss rates) because both are key ingredients for massive star evolution, which determines the final structure of the star. In general the iron core mass shows an overall trend to increase with increasing initial stellar mass, although there is small scale non–monotonic variation of the relation between the iron core and initial stellar mass (Barkat & Marom 1990; Timmes et al. 1996, see their Fig. 4).

Heger et al. (2003) presented a schematic diagram of the fate of compact objects and of supernova types in terms of initial stellar mass and metallicity. For low metallicity stars, the compact objects are, from small to large initial stellar mass, neutron star ($< 25 M_\odot$) – black hole by fallback ($< 40 M_\odot$) – direct black hole ($< 140 M_\odot$) – no remnant due to pair–instability supernova ($< 260 M_\odot$) – direct black hole ($> 260 M_\odot$). This scheme is

modified for stars with high mass loss rates, i.e. higher metallicity and high mass ($> 25 M_{\odot}$), because high mass loss creates smaller helium cores compared with stars of the same mass but with lower metallicity. For higher metallicity stars, the fate of the collapse becomes a function of both the initial stellar mass and the metallicity. For example, a star with a mass of $60 M_{\odot}$ is argued by Heger et al. (2003) to form a black hole directly if the metallicity is low, but a black hole by fallback for intermediate metallicity, and a neutron star for metallicity even larger than the solar value. For stars in the lower mass range ($10 < M_{\odot} < 25$), mass loss is not severe, the fate of compact objects does not depend on metallicity, and the outcome is predicted to always be a neutron star. Therefore, in terms of initial stellar mass and metallicity, our model of a $15M_{\odot}$ star should produce a neutron star regardless of its metallicity.

There is a reasonable case to be made that rotation is involved with the explosion mechanism due to circumstantial evidence from pre-collapse (stellar evolution) and post-explosion (pulsar rotation) phases. The axisymmetric morphology of many supernova nebulae such as the rings of SN 1987A is also considered to be associated with a rotational axis (Wang et al. 2002). Although hydrodynamical instabilities ($\ell = 1$ mode) alone can generate an axisymmetric asphericity (Foglizzo 2002; Blondin et al. 2003), the existence of rotation may inhibit the growth or otherwise modify the nature of the instability (Blondin et al. 2003). Models without rotation cannot explain pulsar activity, so core collapse models with some amount of angular momentum are clearly required. Despite the indication that rotation accompanies core collapse, it is difficult to quantify the amount of angular momentum in the pre-collapse iron core and in the newly born proto neutron star (PNS) since current observations in electromagnetic waves are not capable of revealing that quantity (except perhaps indirectly by polarization). Perhaps detection of gravitational waves from core collapse supernovae will bring progress on this issue (Ott et al. 2004; Müller et al. 2004, and references therein).

We argue that rotation should be a third parameter along with the initial stellar mass and metallicity that rules the nature of the explosion and the fate of the compact objects. Rotation is an important ingredient in stellar evolution where it can affect the mass loss rates, the nuclear evolution through meridional mixing, and the collapse dynamics (Heger et al. 2003; Hirschi, Meynet, & Maeder 2004, and references therein). In our parametric study of rotating core collapse models, we have shown that the resulting rotational velocity of the PNS is very likely to be a non-monotonic function of initial rotational velocity (Fig. 5). The peak of the maximum rotational velocity naturally happens at the boundary separating conditions for which the collapsed core bounces at over nuclear density from conditions resulting in bounce at sub-nuclear density. The model at the peak post-bounce angular velocity possesses a large angular momentum with a compact high-density core. This non-monotonic behavior could have consequences for the explosion and for the fate of the resulting

compact object.

We extend this reasoning to argue that the role of magnetic fields will also depend non-monotonically on the initial iron core rotation. Akiyama et al. (2003) demonstrated that the core collapse environment is prone to the MRI, which amplifies seed magnetic fields to a strength of $\sim 10^{15}$ G. Kotake et al. (2004) and Yamada & Sawai (2004) performed two-dimensional MHD core collapse simulations, and their initial fields (10^{9-12} G) are amplified to $\sim 10^{13-16}$ G due to linear wrapping of the magnetic fields from the attendant differential rotation. Magnetic fields of this strength can affect the explosion via viscous heating (Thompson et al. 2005) and/or by dynamical MHD jets (Kotake et al. 2004; Yamada & Sawai 2004). The effects on the equation of state are estimated to be negligible nearby the PNS where the density is high (H. Duan 2004, private communication; Akiyama et al. 2004), but if a highly magnetic bubble is convected to a low density region, there could be important effects. There could also be an effect on the neutrino cross section (Lai 2001; Bhattacharya & Pal 2002; Duan & Qian 2004).

If jets are necessary for an explosion to occur, then the possibility exists that cores with low initial rotation fail to produce an explosion and hence yield black holes, either directly or by fall-back if the explosion is weak. Peak post-bounce angular velocity could then represent the region of maximum shear, maximum MRI dynamo, maximum affect on neutrino transport and hence maximum explosion strength, guaranteeing a left-over neutron star. Even higher initial rotation with less final rotation and shear could yield weaker magnetic fields and other effects and could yield black hole formation once again. Some fraction of the latter could then yield gamma-ray bursts for more massive progenitor stars. The exact effects of this non-monotonic behavior could depend on the mass and metallicity of the progenitor. In this hypothetical scheme it is not clear where magnetars arise. We note that magnetars are characterized by their large dipole fields that are some, possibly complex, remnant of the post-bounce toroidal fields expected to be generated by the MRI and other related effects. We return to the origin of magnetars below.

Although dynamical effects of magnetic fields are not included in this study, corresponding magnetic field strengths were calculated for each rotational model from m0.1 to m8.0. We have adopted the fiducial saturation model of Akiyama et al. (2003) using their eq. (8),

$$B_{sat}^2 = 4\pi\rho r^2\Omega^2, \quad (12)$$

with an exponential growth timescale of

$$\tau = 4\pi \left| \frac{N^2}{2\Omega} + \frac{d\Omega}{d \ln r} \right|^{-1}. \quad (13)$$

This is the timescale of the maximum growing mode of the linear MRI for the case with entropy gradients (Akiyama et al. 2003).

In these models, the initially small seed fields are amplified near the core bounce due to the strong shear generated by the rapidly rotating compact PNS core and accreting material. We note that the linear stability analysis is local, however, and the MRI has not been established in a dynamical background environment where the radial inflow velocity is faster than the rotational velocity during core collapse. Therefore the evolution of the field strength before the core bounce may not reflect the true effects of the MRI. Once the core has halted collapse and accreting matter inside the shock has a slow radial infall velocity, the MRI linear stability analysis is valid (Akiyama et al. 2003, see their Fig. 15); this pertains after core bounce when the structure is in a quasi-steady state. The field in a given mass zone can evolve somewhat after bounce even in these dissipationless calculations as a given zone expands or contracts, conserving flux.

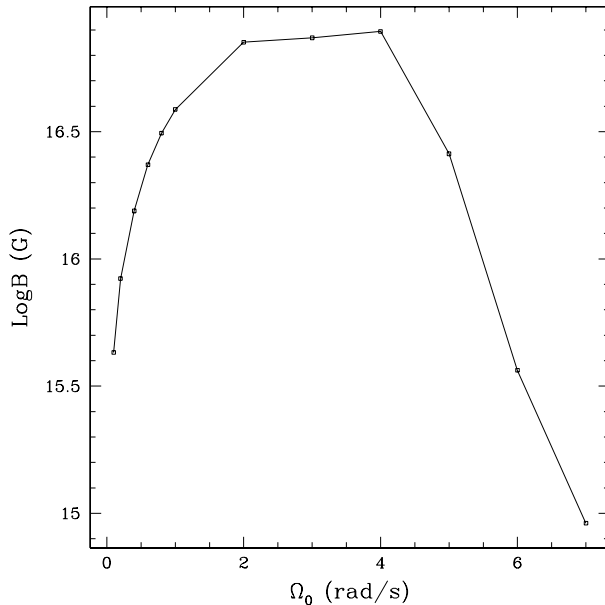


Fig. 6.— Magnetic field strengths for mass shells at the boundary of the PNS core at ~ 30 ms after bounce of the respective runs as a function of initial angular velocity. The non-monotonicity in rotational velocity is reflected in the magnetic field strength as well.

The non-monotonic behavior of rotational velocity is also reflected in the magnetic field strength. The peak of the rotational velocity was found to occur for model m4.0, which also corresponds to the highest estimated value of the magnetic field at bounce. The final saturation field strength grows with Ω_0 up to model m3.0 and then decreases for the models

with more rapid rotation that bounce at sub-nuclear densities (Fig. 6). For models m0.1 through m7.0, the final saturation fields range between $10^{15} - 10^{17}$ G, corresponding to a range of a factor of 10^4 in quantities like the magnetic pressure and hoop stress that depend on the square of the field strength. Even the slow rotating models reach magnetic field strengths of order 10^{15} G in tens of milliseconds. The peak field strengths, $\sim 10^{17}$ G, are nearly large enough to be of direct dynamical importance.

Our simulations only ran at most to ~ 500 msec after the beginning of collapse. This is comparable to the expected explosion timescale, but we note that there is a critical phase yet to come, the de-leptonization phase, lasting perhaps 10 s, during which the rotating PNS will contract and spin up substantially as it becomes a full-fledged neutron star. This phase could be a phase of renewed MHD vigor that we have not explored. If collapse to a black hole does not occur during this phase, then there is a renewed chance of generating even stronger magnetic fields by means of the MRI and hence of driving MHD jets or other processes that can affect the outcome of the supernova. Note that this possibility of renewed MHD activity occurs as the potential for neutrinos to affect the explosion diminishes.

If the supernova is successful, the de-leptonization phase will be followed by a phase of neutron star spindown by magnetic dipole radiation and gravitational wave radiation (Ostriker & Gunn 1969) for the case of typical neutron stars, and by magnetic braking for the case of magnetars (Thompson et al. 2004). These are important epochs for the birth of neutron stars, in which the transition is made from the fury of core collapse to the neutron stars we observe today after the supernova has cleared. The critical nature of this transition phase motivates investigations of the origin and evolution of magnetic fields and rotation (Thompson & Duncan 1993; Thompson & Murray 2001) and their effects on neutrino-driven winds (Thompson et al. 2004), on neutron star recoil mechanisms (Lai et al. 2001), on nucleosynthesis yields, and more.

An important issue is how to make the connection between the rapidly rotating models we describe here and the “normal” pulsars that have modest rotations and Crab-like dipole fields. While some pulsars may be born rotating as fast as a few ms, others may be born rotating more slowly. Examples are the 65 ms pulsar in G11.2-0.3, the remnant of SN 386 (Torii et al. 1997), and the 66 ms pulsar in 3C 58, the remnant of SN 1181 for which Murray et al. (2002) estimate an initial spin of 60 ms. The crucial issue is that the “initial spin” for a pulsar astronomer is the “final spin” for a supernova dynamicist, the spin after the supernova has cleared away. In the jet-driven hypothesis, the rotation of the newborn neutron star represents the fly-wheel that provides the rotational energy to drive the (perhaps magnetically-catalyzed) jets. In this picture, the supernova kinetic energy results in significant part by spinning down the neutron star. Pulsars with relatively long “initial”

rotation periods might then result from neutron stars that had done an especially efficient job of dumping their rotational energy into the expansion energy of the supernova ejecta.

One of the processes that could enhance the depletion of the angular momentum of the neutron star is the formation of a bar with the attendant generation of dynamic, MHD, and gravitational waves. When differential rotation is strong, the value of $T/|W|$ for onset of non-axisymmetric instabilities is substantially decreased (Shibata et al. 2002, 2003; Saijo et al. 2003; Watts et al. 2005). Ott et al. (2005) showed that spiral and bar-like modes can develop in a new-born PNS at $T/|W| \sim 0.08$. If the threshold for instability is low, this mechanism may apply to a wide range of rotating core-collapse models. For the current calculations (c.f. Fig. 5), all the models with initial angular velocity in excess of about 3 s^{-1} , that is, all the most rapidly rotating PNSs could be subject to these instabilities. We note that the timescale for MRI-generated fields to saturate, $\sim 10 \text{ ms}$, may be somewhat shorter than the time for the bar to fully develop, $\sim 50 - 100 \text{ ms}$ (Ott et al. 2005), so that the production of magnetic fields and the growth of the bar would be substantially separate phases in the evolution of a rapidly-rotating PNS. If a bar instability causes a loss of angular momentum, then PNSs may spin down to just the angular momentum at which they achieve stability. There may thus be a tendency for pulsars to be born with just that angular momentum that represents the critical value of $T/|W|$ for developing a bar mode. In practice, this limit may be a function of PNS conditions, the de-leptonization phase must also be considered, and other physical processes can contribute to loss of angular momentum. A great deal of work must be done to get to the point where we can confirm or deny these various possibilities, but the goal of connecting the rotational and magnetic condition of new-born neutron stars to the observed properties of pulsars is of paramount importance.

Another critical issue in the attempt to understand the rotational and magnetic state of new-born neutron stars is the origin and evolution of magnetars. The field strengths we derive for these models are reminiscent of, and even exceed, the fields associated with magnetars. On the other hand, it is very important to bear in mind that the fields generated by the MRI will be strongly toroidal and will be maximal near the boundary of the PNS. The fields associated with magnetars are the poloidal, dipole, components of the neutron star thousands of years later. Also, since the angular velocity gradient is positive deep within the PNS at the time of bounce, the resulting toroidal magnetic field profile is not anchored deep inside the PNS. This means the large fields that the MRI can develop in tens of milliseconds may be especially easy to shed as the surrounding material dissipates in the supernovae explosion. We point out that the magnetar dipole field may not be generated by the MRI, but generated within the PNS core by an efficient $\alpha - \Omega$ dynamo as suggested by Thompson & Duncan (1993) after spin down of the PNS due to de-leptonization. The condition for an efficient $\alpha - \Omega$ dynamo requires rapid rotation so that the Rossby number,

the ratio of the rotation time to the convective time, is small, nearly unity (Duncan & Thompson 1992; Thompson & Duncan 1993). Because of the non-monotonic dependence of the final rotational velocity on initial iron core rotation, magnetar progenitors may not correspond to the most rapidly rotating iron cores, but to iron cores with some intermediate initial rotational velocity. In addition, the condition to drive an $\alpha - \Omega$ dynamo may not arise during the explosion of the supernova, but during or after the contraction of the PNS due to de-leptonization. At core bounce, model m4.0 has a rotational period of ~ 1.7 msec at the boundary of the PNS core. If we consider spin up of the core by contraction at a later time, this model may be able to provide the rapid rotation needed for an efficient $\alpha - \Omega$ dynamo, hence giving rise to magnetar magnetism. The condition to produce magnetar dipole fields, like the condition to maximize the rotation and the field strength in a way to maximally promote a supernova explosion, suggests that making an MHD jet-induced (or jet-aided) supernova and producing a magnetar may require conditions near the peak in the non-monotonic, post-collapse, rotation rates that we emphasize here. The fact that the most energetic supernova explosions may require maximal effect of the MRI, and that magnetars may require maximal effect of the $\alpha - \Omega$ dynamo means that the conditions for these sets of outcomes may not be identical. Leaving behind a magnetar requires a successful supernova explosion, but the opposite need not be true. Thus, the channel for the production of magnetars must be a subset of the conditions that give successful supernovae. Future study may reveal which range of initial iron core rotation rates yields successful supernovae, and which conditions within that range yield magnetars.

We thank I. Lichtenstadt for his generosity in supplying the code, and P. Höflich and E. L. Robinson for helpful discussion. We also thank the anonymous referee for useful comments. This work was supported in part by NASA Grant NAG59302 and NSF Grant AST-0098644.

REFERENCES

- Akiyama, S., Wheeler, J. C., Meier, D. L., & Lichtenstadt, I. 2003, *ApJ*, 584, 954
- Akiyama, S., Wheeler, J. C., Meier, D. L., & Duncan, R. C. 2004, in *Cosmic Explosions in Three Dimensions*, eds. P. Höflich, P. Kumar, & J. C. Wheeler (Cambridge: Cambridge University Press), in press
- Balbus, S. A. & Hawley, J. F. 1998, *Review of Modern Physics*, 70, 1
- Barkat, Z. & Marom, A. 1990, *Supernovae*, Jerusalem Winter School for Theoretical Physics, 95

- Bhattacharya, K., & Pal, B. 2002, preprint (hep-ph/0209153)
- Blondin, J. M., Mezzacappa, A., & DeMarino, C. 2003, *ApJ*, 584, 971
- Burrows, A. 1988, *ApJ*, 334, 891
- Duan, H., & Qian, Y. -Z. 2004, *Phys. Rev. D*, 69, 123004
- Duncan, R. C. & Thompson, C. 1992 *ApJ*, 392, L9
- Foglizzo, T. 2002, *A&A*, 392, 353
- Fryer, C. L. 1999, *ApJ*, 522, 413
- Fryer, C. L. & Heger, A. 2000, *ApJ*, 541, 1033
- Fryer, C. L. & Kalogera, V. 2001, *ApJ*, 554, 548
- Fryer, C. L. & Warren, M. S. 2004, *ApJ*, 601, 391
- Heger, A., Fryer, C. L., Woosley, S. E., Langer, N., & Hartmann, D. H. 2003, *ApJ*, 591, 288
- Hirschi, R., Meynet, G., & Maeder, A. 2004, *A&A*, 425, 649
- Höflich, P., Khokhlov, A., & Wang, L. 2001, in *Proc. of the 20th Texas Symposium on Relativistic Astrophysics*, eds. J. C. Wheeler & H. Martel (New York: AIP)
- Khokhlov, A. M., Höflich, P., Oran, E. S., Wheeler, J. C., Wang, L., & Chtchelkanova, A. Yu. 1999, *ApJ*, 524, L107
- Khokhlov, A. & Höflich, P. 2001, in *AIP Conf. Proc. No. 556, Explosive Phenomena in Astrophysical Compact Objects*, eds. H.-Y. Chang, C.-H. Lee, & M. Rho (New York: AIP), 301
- Kotake, K., Sawai, H., Yamada, S., & Sato, K. 2004, *ApJ*, 608, 391
- Kouveliotou, C., Strohmayer, T., Hurley, K., van Paradijs, J., Finger, M. H., Dieters, S., Woods, P., Thomson, C., & Duncan, R. C. 1999, *ApJ*, 510, L115
- Lai, D. 2001, *Rev. Mod. Phys.*, 73, 629
- Lai, D., Chernoff, D. F. & Cordes, J. M. 2001, *ApJ*, 549, 1111
- Langer, N. 2004, in *Cosmic Explosions in Three Dimensions*, eds. P. Höflich, P. Kumar, & J. C. Wheeler (Cambridge: Cambridge University Press), p. 191

- Lattimer, J. M., & Swesty, F. D. 1991, *Nucl. Phys. A*, 535, 331
- Leonard, D. C., Filippenko, A. V., Barth, A. J., & Matheson, T. 2000, *ApJ*, 536, 239
- Leonard, D. C., Filippenko, A. V., Ardila, D. R., & Brotherton, M. S. 2001, *ApJ*, 553, 861
- Leonard, D. C., Filippenko, A. V., Chornock, R., & Foley, R. J. 2002, *PASP*, 114, 1333
- Liebendörfer, M., Thielemann, F. -K., Messer, O. E. B., Hix, W. R., & Bruenn, S. W. 2001a, *Phys. Rev. D*, 63, 103004
- Liebendörfer, M., Mezzacappa, A., & Thielemann, F. -K. 2001b, *Phys. Rev. D*, 63, 104003
- Maeda, K. & Nomoto, K. 2003, *ApJ*, 598,1163
- Mezzacappa, A., Liebendörfer, M., Messer, O. E. B., Hix, W. R., Thielemann, F. -K., & Bruenn, S. W. 2001, *Phys. Rev. Lett.*, 86, 1935
- Mönchmeyer, R. & Müller, E. 1989, in *Timing Neutron Stars*, ed. H. Ögelman & E. P. J. van den Heuvel (NATO ASI Ser. C, 262; New York: ASI), 549
- Müller, E., Rampp, M., Buras, R., & Janka, H. -T. 2004, *ApJ*, 603, 221
- Murray, S. et al. 2002, *ApJ*, 568, 226
- Myra, E. S., Bludman, S. A., Hoffman, Y., Lichtenstadt, I., Sack, N., & van Riper, K. A. 1987, *ApJ*, 318, 744
- Ostriker, J. P. & Gunn, J. E. 1969, *ApJ*, 157, 1395
- Ott, C. D., Burrows, A., Livne, E., & Walder, R. 2004, *ApJ*, 600, 834
- Ott, C. D., Ou, S., Tohline, J. E., & Burrows, A. 2005, *astro-ph/0503187*
- Rampp, M., & Janka, H. -Th. 2000, *ApJ*, 539, 33
- Rampp, M., & Janka, J. -Th. 2002, *A&A*, 396, 361
- Saijo, M., Baumgarte, T. W., & Shapiro, S. L. 2003, *ApJ*, 600, 352
- Shibata, M., Karino, S., & Eriguchi, Y. 2002, *MNRAS*, 334, L27
- Shibata, M., Karino, S., & Eriguchi, Y. 2003, *MNRAS*, 343, 619
- Shapiro, S. L. & Teukolsky, S. A. 1983, *Black Holes, White Dwarfs, and Neutron Stars* (New York: John Wiley & Sons)

- Tassoul, J. -L. 1978, *Theory of Rotating Stars* (Princeton: Princeton University Press)
- Thompson, C. & Duncan, R. C. 1993, *ApJ*, 408, 194
- Thompson, C. & Murray, N. 2001, *ApJ*, 560, 339
- Thompson, C. & Murray, N. 2002, preprint (astro-ph/0105425)
- Thompson, T. A., Burrows, A., & Pinto, P. A., 2003 *ApJ*, 592, 434
- Thompson, T. A., Chang, P., & Quataert, E. 2004, *ApJ*, 611, 380
- Thompson, T. A., Quataert, E., & Burrows, A. 2005, *ApJ*, 620, 861
- Timmes, F. X., Woosley, S. E., & Weaver, T. A. 1996, *ApJ*, 457, 834
- Torii, K., Tsunemi, H., Dotani, T. & Mitsuda, K. 1997, *ApJ*, 489, L147
- Wang, L., Wheeler, J. C., Li, Z. W., & Clocchiatti, A. 1996, *ApJ*, 467, 435
- Wang, L., Howell, D. A., Höflich, P., & Wheeler, J. C. 2001, *ApJ*, 550, 1030
- Wang, L., Wheeler, J. C., Höflich, P., Khokhlov, A., Baade, D., Branch, D., Challis, P., Filippenko, A. V., Fransson, C., Garnavich, P., Kirshner, R. P., Lundqvist, P., McCray, R., Panagia, N., Pun, C. S. J., Phillips, M. M., Sonneborn, G., & Suntzeff, N. B. 2002, *ApJ*, 579, 671
- Wang, L., Baade, D., Höflich, P., & Wheeler, J. C. 2003, *ApJ*, 592, 457
- Watts, A. L., Andersson, N., & Jones, D. I. 2005, *ApJ*, 618, L37
- Wheeler, J. C., Yi, I., Höflich, P., & Wang, L. 2000, *ApJ*, 537, 810
- Wheeler, J. C., Meier, D. L., & Wilson, J. R. 2002, *ApJ*, 568, 807
- Yamada, S. & Sawai, H. 2004, *ApJ*, 608, 907